DALTON
FULL PAPER

Ligand exchange and stereodynamics in the cationic palladium(II)–π-allyl complex of 2,2′-bis(pyridyl)-1,1′-binaphthalene, a novel atropisomeric *N,N*-ligand

Jonathan P. H. Charmant,[a] Ian A. Fallis,[b] Neil J. Hunt,[a] Guy C. Lloyd-Jones,*[a] Martin Murray[a] and Thorsten Nowak[c]

[a] *School of Chemistry, Cantock's Close, Bristol, UK BS8 1TS. E-mail: guy.lloyd-jones@bris.ac.uk*
[b] *School of Chemistry, University of Wales at Cardiff, PO Box 912, Cardiff, UK CF10 3TB*
[c] *AstraZeneca Pharmaceuticals, Mereside, Alderley Park, Macclesfield, Cheshire, UK SK10 4TG*

Received 24th January 2000, Accepted 4th April 2000
Published on the Web 4th May 2000

Racemic 2,2′-bis(pyridin-2-yl)-1,1′-binaphthalene (±)-**6** was prepared in four synthetic steps from 2-naphthol. Resolution of the novel atropisomeric ligand **6** was effected by repeated preparation, recrystallisation and then liberation of the bis-tartrate salt (D and L). This affords both enantiomers of **6** (>96% enantiomeric excess, ee) whose absolute configurations were assigned by CD. The ligand **6** is stable towards racemisation ($\Delta G^{\ddagger}_{rac}$ > 167 kJ mol^{-1}) and the structure was confirmed by single crystal X-ray diffraction of the complex [$ZnCl_2$(**6**)]. The structure and stereodynamics of the complex [Pd(η^3-C_3H_5)(**6**)][OTf] (OTf = O_3SCF_3) which comprises a C_2-symmetric ligand bound *via* Pd to a non-C_2-symmetric allyl fragment was studied in detail in solution by 1-D and 2-D ^{1}H NMR and in the solid state by single crystal X-ray diffraction. Apparent stereodynamic processes of the allyl ligand, as detected in solution by NMR, are shown to arise from ligand **6** stereodynamics and exchange. The ligand **6** represents the first compound/building block for a series of enantiomerically pure *N,N*-ligands that may be of utility in supramolecular co-ordination chemistry and in asymmetric catalysis.

Introduction

The design, synthesis and application of novel chiral ligand structures continues to be an area of great activity and interest to inorganic and organic chemists alike.[1] Ligand bite angle, electronic and steric symmetry and asymmetry, shape and depth of 'chiral pocket', ease of synthesis and availability of both enantiomers are some of the features generally identified as pertinent ligand design considerations for asymmetric catalysis. In this arena, the importance of ligands based on the atropisomeric 1,1′-binaphthalene skeleton **1** is indisputable and within this class there is a vast range of ligands that have been prepared and studied. Arguably, the most renowned ligand in this series is 2,2′-bis(diphenylphosphino)-1,1′-binaphthalene ('BINAP') **2**[2] which, as an electronically symmetrical P,P ligand, has seen an enormous range of highly successful applications to asymmetric catalysis. Phosphines aside, there are also a range of electronically symmetrical, chiral, enantiomerically pure C_2-symmetric N,N ligands that have successfully been applied to a variety of asymmetric catalytic processes. Examples include semicorrin ligands **3**,[3] the ubiquitous bis(oxazoline) ligands **4**[4] and bis(aziridine) ligands **5**.[5]

We have an ongoing interest in development of chiral ligands for supramolecular co-ordination chemistry, asymmetric catalysis and crystal engineering and it occurred to us that the incorporation of pyridine or bipyridine units[6] into a 1,1′-binaphthalene skeleton would provide a novel range of ligands that would be potentially useful in these arenas. We chose the simplest system, namely 2,2′-bis(pyridin-2-yl)-1,1′-binaphthalene **6**, as the first target and herein report on its synthesis, resolution and complexation to Pd^{II} and to Zn^{II}.[7] The π-allyl complexes of the former provide for the study of some unusual stereodynamic processes.

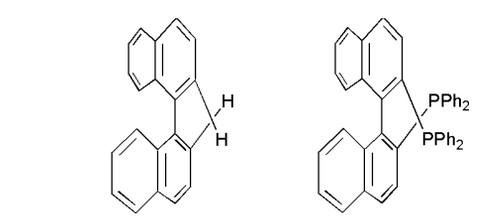

M-**1** (a*R*) a*R* (+)-*M*-**2**

3 **4**

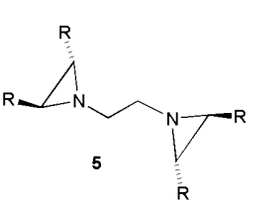

5

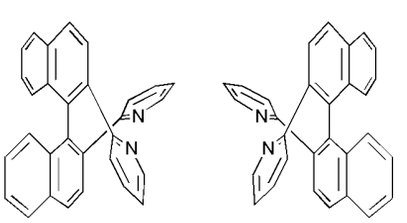

M-**6** (a*R*) *P*-**6** (a*S*)

Results and discussion

Synthesis

To prepare 2,2′-bis(pyridyl)-1,1′-binaphthalene **6** we considered two general strategies (**A** and **B**, Scheme 1). Strategy **A**

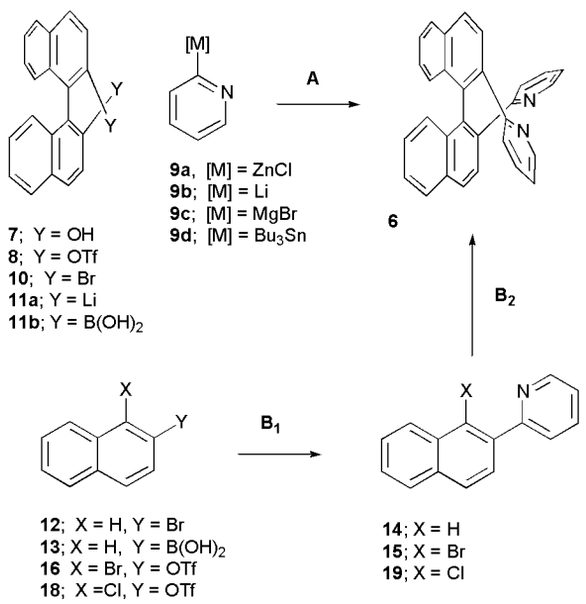

Scheme 1 The two basic strategies (**A** and **B**) considered for the preparation of compound **6**.

has the advantage that a number of binaphthalene compounds functionalised at the 2,2′ positions are known and are readily resolved or commercially available in enantiomerically pure form. Furthermore, transition-metal mediated or catalysed cross-coupling would provide a range of methods for construction of the pyridyl-to-naphthalene bonds. Strategy **B**, on the other hand, suffers the requirement for resolution (unless an enantioselective coupling procedure is devised) but does allow construction of the pyridylnaphthalene unit without the problems associated with the steric bulk of the binaphthalene.

Strategy **A** appeared preferable and (±)-2,2′-binaphthol **7**[8] was converted into ditriflate **8** (OTf = O_3SCF_3). However, this failed to undergo Pd-catalysed cross-coupling with chloro (2-pyridyl) zinc **9a**, as did dibromide **10**[9,†] with a range of 2-metallopyridine reagents **9a**–**9d** under both palladium or nickel-catalysis. Reversing the cross-coupling polarities was then attempted by conversion of the dibromide **10** into the corresponding 1,1-binaphthalene bis-lithio and bis-boronic acid derivatives **11a**, **11b**. However, an attempted [1,2] addition of **11a** to pyridine followed by oxidative rearomatisation[10] failed to proceed cleanly and both **11a** and **11b** failed to couple with two equivalents of 2-bromopyridine under a variety of Pd-catalysed conditions. A model study in which 2-bromonaphthalene **12** was converted into the corresponding boronic acid **13** readily furnished 2-pyridin-2-ylnaphthalene **14** by Pd-catalysed cross-coupling with 2-bromopyridine (Scheme 1). This seemed to suggest that strategy **A** was not promising, presumably due to complications in effecting addition of two pyridines to the binaphthalene framework ‡ and thus we moved to strategy **B** (**B**$_1$ and **B**$_2$, Scheme 1).

A reductive (dehalogenative) coupling method seemed a reasonable starting point for strategy **B**$_2$ and we therefore attempted to prepare 1-bromo-2-(pyridin-2-yl)naphthalene **15**. We chose to employ the conditions recently reported[11] for highly selective cross-coupling of aryl triflates in the presence of aryl bromides (Scheme 2). In Hayashi's example PhMgBr was successfully mono-cross-coupled ([Pd(dppp)Cl_2], 5 mol%) with 1-bromo-2-trifluoromethylsulfonyloxynaphthalene **16** to afford 1-bromo-2-phenylnaphthalene **17** in good yield.

In our case, reaction with 2-metallopyridyl reagents **9a** or **9c** ([M] = ZnCl or BrMg) under identical conditions to those reported[11] resulted in very low conversion and the bulk of bromotriflate **16** was recovered unreacted. However, we did obtain traces of the desired bromopyridyl **15** and *debrominated* cross-coupled product **14**. It therefore seems that either co-ordination of the Pd to the pyridyl group in **15** allows oxidative insertion into the Ar–Br bond and this then terminates catalysis, or the pyridyl group facilitates magnesium- or zinc-halide exchange. In either case, acidic work-up hydrolyses the [M]–Ar bond to give **14**. This intramolecular assistance is not available with the 2-phenylated compound **17**,[11] Scheme 2. Knowing that oxidative insertion of Pd^0 into Ar–Cl bonds[12] is much slower than into the corresponding Ar–Br we prepared chlorotriflate **18** from 1-chloro-2-naphthol§ and then obtained, under identical conditions, the desired 1-chloro-2-(pyridin-2-yl)naphthalene **19** in good yield (82%). Using the Iyoda modification[13] of the Colon procedure,[14] Ni-mediated dehalogenotative reductive homocoupling of **19** afforded the desired ligand (±)-**6** in 69% yield on a 2 g scale. Although (±)-**6** is crystalline (mp 163–165 °C), we were unable to grow single crystals of suitable dimensions for X-ray diffraction.

Complexation and resolution

To study the potential of compound **6** to function as a ligand, we performed a series of ^{1}H NMR experiments in which a solution of **6** (0.02 M) in d_3-acetonitrile was titrated with a solution of $ZnCl_2$ (0.90 M) in d_3-acetonitrile. Aliquots of the $ZnCl_2$ solution comprising *ca*. 0.25 equivalent Zn per **6** were added in increments until a total of 2 equivalents had been added. Prior to addition of a total of one equivalent of $ZnCl_2$, two sets of ^{1}H NMR signals were observed, one corresponding to a complex **20** (in which a set of ten ^{1}H NMR multiplet signals (each integrating for 2 H) were apparent) and the other corresponding to the "free" ligand **6**. The mol fraction of **20** in the mixture of **20** and **6** was directly proportional to the equivalents of $ZnCl_2$ that had been added. There was no signal broadening above natural line width for either **6** or **20**. After addition of a full equivalent of $ZnCl_2$ all signals due to **6** had disappeared and on addition of further $ZnCl_2$ there was no change in linewidth of signals due to the complex **20**. These results confirm that (a) bis-pyridyl compound **6** can act as a ligand towards zinc, (b) that the complex **20** thus formed involves fully, or time-averaged, C_2-symmetrical bidentate co-ordination of Zn, (c) exchange of $ZnCl_2$ between the complex **20** and "free" ligand **6** is below the NMR timescale and (d) complexes of type [$ZnCl_2$(**6**)$_2$], in which **6** acts as a monodentate ligand, are not present to any significant extent.

† Although the conversion of binaphthol **7** into the corresponding dibromide **10** is a literature procedure we had great problems reproducing the reaction on a small scale. Furthermore, the vigorous conditions (2 equivalents Ph_3PBr_2 per **7** then heat from 25 to 350 °C) effects racemisation and thereby negates one of the prime motives for employing route **A**. Attempted oxidative (dehydrogenative) homocoupling of 2-bromonaphthalene by stoichiometric use of $Pb(OAc)_4$ (as extensively developed by McKillop, see *e.g.*: A. McKillop, A. G. Turrell, D. W. Young and E. C. Young, *J. Am. Chem. Soc.,* 1980, **102**, 6504) failed to give **10**.

‡ We did succeed in the introduction of one pyridine onto compound **11b** (Pd-catalysed Suzuki reaction with 2-bromopyridine) to generate what we have tentatively assigned (based on MS) as 2-(pyridin-2-yl)-1,1′-binaphthyl-2′-boronic acid. In line with observations made by B. Schilling and D. E. Kaufman, *Eur. J. Org. Chem.*, 1998, 701, this failed to undergo a second cross-coupling.

§ 1-Chloro-2-naphthol is readily prepared *via* regioselective chlorination (*t*-BuOCl) of 1-naphthol, see: D. Ginsberg, *J. Am. Chem. Soc.*, 1951, **73**, 2723.

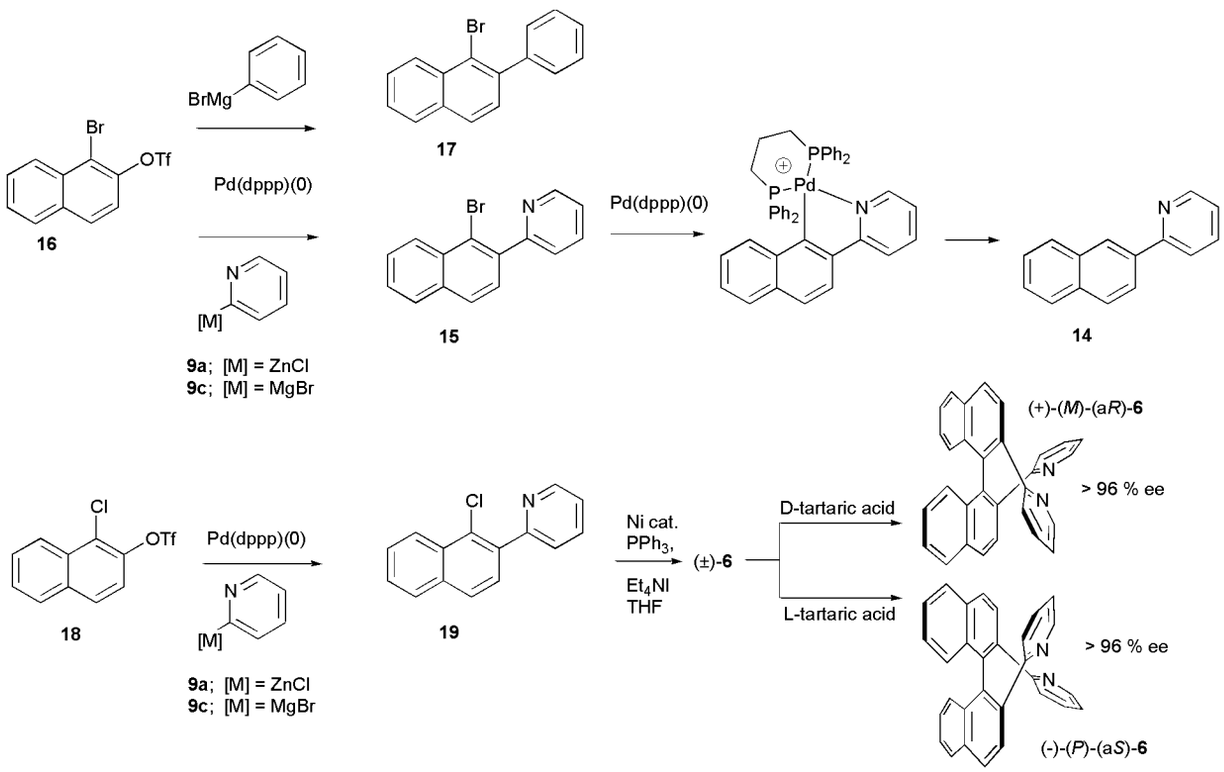

Scheme 2 Highly selective Pd-catalysed cross-coupling of triflates in the presence of halides that were employed in the preparation of compound **6**.

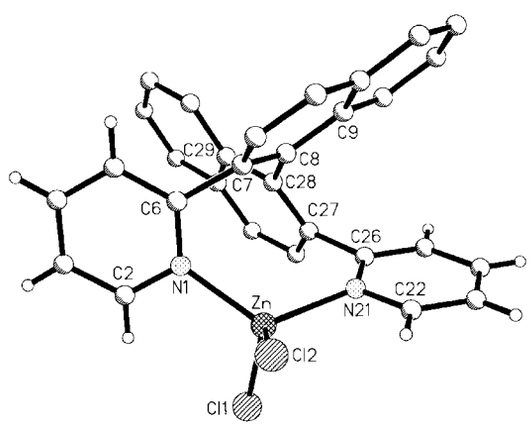

Fig. 1 The molecular structure of complex **20** ([$ZnCl_2$(**6**)]) in the crystal.

When performed on a larger scale, complex (±)-**20** could be prepared in analytically pure form in 70% yield (mp > 300 °C). Crystallisation from acetonitrile gave blocks that were suitable for single crystal X-ray diffraction, Fig. 1. The structure of (±)-**20** reveals a tetrahedral zinc complex with two chloride ligands and the chelating dipyridylbinaphthyl ligand **6**. Selected bond lengths and angles are given in Table 1. The molecule crystallises as a racemic mixture in the centrosymmetric space group $P2_1/c$. The length of the bond between sp^2 carbons C(8) and C(28) [1.504(2) Å] results from the twisted conformation of the naphthalene rings [torsion angle C(9)–C(8)–C(28)–C(29) 103.2°] which prevents delocalisation of electron density between the rings *via* this bond. The conformation of the ligand **6** is dictated by this angle and the near identical torsion angles around the C(6)–C(7) and C(26)–C(27) bonds [N(1)–C(6)–C(7)–C(8) −66.8 and N(21)–C(26)–C(27)–C(28) −65.6°].

Having satisfied ourselves that, as planned, compound **6** can function as a bidentate ligand, we began to study methods for resolution of the enantiomers from the racemate. Choosing to exploit the basic nature of the pyridyl groups we prepared diastereomeric salts with tartaric acid.¶ Repeated formation, precipitation then liberation of the ligand **6** from the tartrate salt yielded *ca.* 0.6 g samples of (+)-**6** and (−)-**6**. To analyse the enantiomeric enrichment, we developed a ^{1}H NMR assay using a chiral lanthanide shift reagent ((+)-Eu(hfc)$_3$, hfc = heptafluoropropylcamphorate) to resolve the protons at the 6,6′ positions‖ (C(2)–H and C(22)–H in Fig. 1). Extrapolation to zero of a calibration plot obtained by integration after addition of 0, 1, 2 and 3 mol% of racemic (±)-**6** to the sample of (−)-**6** suggested that the enantiomeric purity of the two samples of resolved **6** was >98% (>96% ee) in both cases.

To assign the absolute configuration we employed circular dichroism. Here, the well known and very large Cotton effects induced by binaphthalene rings[15] established that the chiral

¶ Of the readily available enantiomerically pure chiral acids tested (lactic, malic, mandelic, camphorsulfonic and tartaric) only tartaric acid effected any enantiomeric enrichment whatsoever. Since tartaric acid is a diacid and ligand **6** a dibase, there are three limiting stoichiometries of combination and finding the correct one (2:1, respectively) and the correct solvent (ethyl acetate) proved crucial in achieving reasonable levels of diastereomeric enrichment. Indeed, 'wrong' combinations led to very low yields of enriched material (<5%). However, under the optimum conditions, we were able to obtain (−)-**6** (58.8% yield, 75% enantiomeric excess, ee) by liberation from the precipitated salt (treatment with NaOH) and (+)-**6** (77.2% yield, 77% ee) from salt remaining in solution after reaction with L-tartaric acid giving a total recovery of 68% **6**. Despite the different melting point and thus crystal habit of racemic *versus* enantiomerically pure **6** (163–165 and 104 °C respectively), precipitation of microcrystals of (−)- or (+)-**6** from hexane failed to upgrade, or even alter, the enantiomeric excess. Furthermore, after the initial resolution, although treatment of (−)-**6** with L-tartaric acid led to precipitation of a salt with de (diastereomeric excess) higher than 75%, the de of the salt remaining in solution was *ca.* 0%. Thus to obtain enantiomerically pure (+)-**6**, we employed D-tartaric acid (unnatural) for this series. Racemic **6** (recovered from (−)-**6** + L-tartaric acid and from (−)-**6** + D-tartaric acid) was recycled using the initial resolution procedure.

‖ These protons were chosen since they are in a clear window of the ^{1}H NMR spectrum. A study of $\Delta\delta$ *versus* equivalents (+)-Eu(hfc)$_3$ displayed a linear relationship. However, at high loadings of Eu(hfc)$_3$ line broadening (ω) became severe and optimum conditions were (+)-Eu(hfc)$_3$, 0.4 equivalent, C_6D_6, $\Delta\delta$ *ca.* 50 Hz.

Table 1 Selected bond lengths (Å) and angles (°) for complex **20**

Zn–N(21)	2.0499(12)	C(14)–C(15)	1.420(2)
Zn–N(1)	2.0513(11)	C(15)–C(16)	1.368(2)
Zn–Cl(2)	2.2341(4)	N(21)–C(22)	1.3480(18)
Zn–Cl(1)	2.2537(4)	N(21)–C(26)	1.3534(18)
N(1)–C(2)	1.3484(18)	C(22)–C(23)	1.381(2)
N(1)–C(6)	1.3501(17)	C(23)–C(24)	1.376(2)
C(2)–C(3)	1.383(2)	C(24)–C(25)	1.383(2)
C(3)–C(4)	1.382(2)	C(25)–C(26)	1.397(2)
C(4)–C(5)	1.382(2)	C(26)–C(27)	1.495(2)
C(5)–C(6)	1.3931(19)	C(27)–C(28)	1.388(2)
C(6)–C(7)	1.4940(19)	C(27)–C(36)	1.421(2)
C(7)–C(8)	1.3859(18)	C(28)–C(29)	1.4341(19)
C(7)–C(16)	1.4180(19)	C(29)–C(30)	1.422(2)
C(8)–C(9)	1.4310(19)	C(29)–C(34)	1.428(2)
C(8)–C(28)	1.5039(18)	C(30)–C(31)	1.373(2)
C(9)–C(10)	1.421(2)	C(31)–C(32)	1.412(3)
C(9)–C(14)	1.4253(19)	C(32)–C(33)	1.355(3)
C(10)–C(11)	1.375(2)	C(33)–C(34)	1.419(2)
C(11)–C(12)	1.414(2)	C(34)–C(35)	1.418(2)
C(12)–C(13)	1.360(2)	C(35)–C(36)	1.361(2)
C(13)–C(14)	1.418(2)		
N(21)–Zn–N(1)	119.52(5)	C(15)–C(14)–C(9)	119.21(13)
N(21)–Zn–Cl(2)	104.86(3)	C(16)–C(15)–C(14)	120.88(13)
N(1)–Zn–Cl(2)	106.56(3)	C(15)–C(16)–C(7)	120.42(14)
N(21)–Zn–Cl(1)	105.01(3)	C(22)–N(21)–C(26)	118.42(12)
N(1)–Zn–Cl(1)	104.30(3)	C(22)–N(21)–Zn	116.60(10)
Cl(2)–Zn–Cl(1)	117.306(15)	C(26)–N(21)–Zn	123.93(9)
C(2)–N(1)–C(6)	118.77(12)	N(21)–C(22)–C(23)	123.08(14)
C(2)–N(1)–Zn	117.68(9)	C(24)–C(23)–C(22)	118.66(14)
C(6)–N(1)–Zn	122.15(9)	C(23)–C(24)–C(25)	119.17(14)
N(1)–C(2)–C(3)	122.88(14)	C(24)–C(25)–C(26)	119.72(15)
C(4)–C(3)–C(2)	118.50(15)	N(21)–C(26)–C(25)	120.90(13)
C(3)–C(4)–C(5)	118.99(14)	N(21)–C(26)–C(27)	118.57(12)
C(4)–C(5)–C(6)	120.05(14)	C(25)–C(26)–C(27)	120.47(13)
N(1)–C(6)–C(5)	120.71(13)	C(28)–C(27)–C(36)	120.33(14)
N(1)–C(6)–C(7)	118.59(12)	C(28)–C(27)–C(26)	120.31(12)
C(5)–C(6)–C(7)	120.64(13)	C(36)–C(27)–C(26)	119.25(13)
C(8)–C(7)–C(16)	120.44(13)	C(27)–C(28)–C(29)	119.65(13)
C(8)–C(7)–C(6)	120.02(12)	C(27)–C(28)–C(8)	120.23(12)
C(16)–C(7)–C(6)	119.40(12)	C(29)–C(28)–C(8)	120.09(12)
C(7)–C(8)–C(9)	119.87(12)	C(30)–C(29)–C(34)	118.46(14)
C(7)–C(8)–C(28)	120.43(12)	C(30)–C(29)–C(28)	122.34(13)
C(9)–C(8)–C(28)	119.69(12)	C(34)–C(29)–C(28)	119.17(14)
C(10)–C(9)–C(14)	118.48(13)	C(31)–C(30)–C(29)	120.98(16)
C(10)–C(9)–C(8)	122.45(13)	C(30)–C(31)–C(32)	120.04(17)
C(14)–C(9)–C(8)	119.06(13)	C(33)–C(32)–C(31)	120.46(16)
C(11)–C(10)–C(9)	120.82(15)	C(32)–C(33)–C(34)	121.41(17)
C(10)–C(11)–C(12)	120.17(16)	C(35)–C(34)–C(33)	122.29(16)
C(13)–C(12)–C(11)	120.35(15)	C(35)–C(34)–C(29)	119.07(14)
C(12)–C(13)–C(14)	121.10(15)	C(33)–C(34)–C(29)	118.63(16)
C(13)–C(14)–C(15)	121.72(14)	C(36)–C(35)–C(34)	121.04(15)
C(13)–C(14)–C(9)	119.08(14)	C(35)–C(36)–C(27)	120.66(15)

binaphthalene axis of the (−)-enantiomer of compound **6** has *P* helicity (*aS* configuration) and thus (+)-**6** has *M* helicity (*aR* configuration).** The barrier to rotation about the atropisomeric axis in 2,2′-disubstituted 1,1′-binaphthalene compounds is usually high enough to confer long term stability towards racemisation. To confirm that this was indeed so for **6**, we heated a solution of it (>96% ee) in ethylene glycol to 170 °C for two days. On cooling and recovery of **6** there was no observable racemisation and thus the barrier to enantiomerisation†† at 443 K is therefore >*ca.* 167 kJ mol^{-1}.

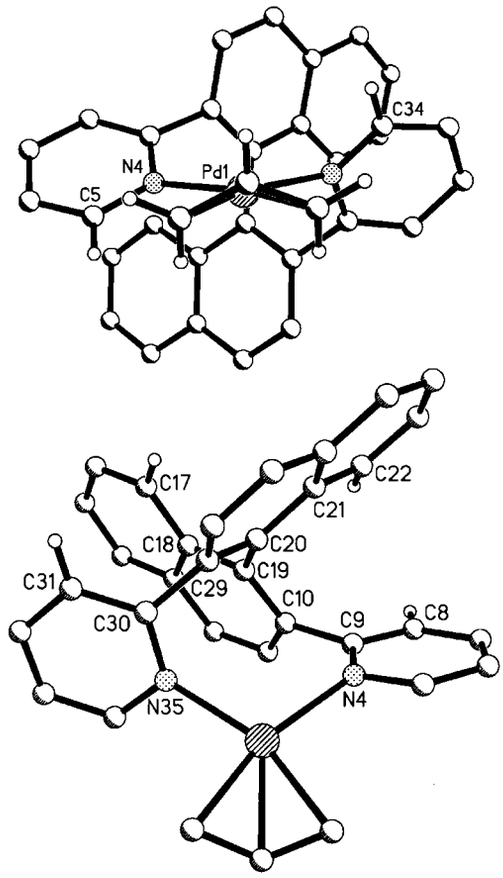

Fig. 2 Two views of the molecular structure of one of the two crystallographically independent molecules in complex (±)-**21** ((±)-[Pd(C_3H_5)(**6**)][OTf]) in the crystal. Upper view: the allyl and pyridyl protons [on C(5) and C(34)] involved in NOE studies of allyl geometry in solution. Lower view: protons on C(31)/C(17) and C(8)/C(22) involved in intraligand NOE. In both views, all other protons are omitted for clarity.

Preparation, crystal structure and solution stereodynamics of complex 21

To study the complexation of compound **6** to Pd we chose to use [Pd(MeCN)$_2$(η^3-C_3H_5)][OTf] as a convenient source of halide-free palladium–allyl. This crystalline complex is readily prepared by AgOTf-mediated chloride abstraction from [Pd_2Cl_2(η^3-C_3H_5)$_2$] in MeCN solution and is stable for long periods when stored at −20 °C. Reaction of [Pd(MeCN)$_2$(η^3-C_3H_5)][OTf] with **6** in CH_2Cl_2 gave the complex [Pd(η^3-C_3H_5)(**6**)][OTf] **21** as bright yellow crystals in 53–71% yields (mp 196 °C) after crystallisation from CH_2Cl_2–Et_2O. Although the analogous enantiomerically pure complexes (−)-**21** and (+)-**21** are equally readily prepared (as pale yellow needles, mp 166–168 °C) we were unable, despite many attempts, to grow high quality crystals of suitable dimensions for X-ray diffraction. In contrast, the racemate (±)-**21** crystallised well. The molecular structure is shown in Fig. 2. Two crystallographically

** We initially attempted to crystallise salts of compound **6** obtained by reaction of either enantiomer with the same range of chiral, enantiomerically pure, acids that we had tested for the resolution, in the hope that we could determine the absolute configuration of **6** by single crystal X-ray diffraction. However, in no case we could obtain crystals of sufficient dimensions or quality. Ironically, the salt obtained by reaction of racemic (±)-**6** with camphorsulfonic acid was readily crystallised (in 0% de). We therefore turned to the potential to use anisotropic scattering. However, despite the ready crystallisation of racemic (±)-[$ZnCl_2$(**6**)] and (±)-[Pd(allyl)(**6**)][OTf], the enantiomerically pure complexes resolutely failed to yield good quality crystals. Notably, the racemic complexes crystallised with heterochiral unit cells.

†† The barrier for binaphthalene itself is *ca.* 100 kJ mol^{-1} giving it a half-life of *ca.* 0.5 s at 160 °C. The rate constant for enantiomerisation may be calculated from the relationship $k = 0.5\{(1/t)\ln[1/(1 - 2x)]\}$ where t = time taken for mol fraction x of enantiomer to be generated from 100% ee sample. If we assume compound **6** to be of 100% ee to start with, then if after heating to 170 °C (443 K) for 48 h (172.8 ks) we could still not detect the opposite enantiomer of **6** (with a limit of detection for *enant*-**6** of 2%), the threshold rate (k_{max}) is below 1.18×10^{-7} s^{-1}. Since $\Delta G_{min} = -RT\{\ln(k_{max}h/kT)\}$, the threshold energy barrier ($\Delta G^{\ddagger}_{min}$) to enantiomerisation may be calculated as 167 kJ mol^{-1} at 443 K.

Table 2 Selected bond lengths (Å) and angles (°) for complex **21**

Pd(1)–C(2)	2.123(4)	C(16)–C(17)	1.364(4)
Pd(1)–C(1)	2.137(3)	C(17)–C(18)	1.428(4)
Pd(1)–C(3)	2.146(3)	C(18)–C(19)	1.426(4)
Pd(1)–N(4)	2.167(2)	C(19)–C(20)	1.501(4)
Pd(1)–N(35)	2.137(3)	C(20)–C(29)	1.392(4)
C(1)–C(2)	1.354(5)	C(20)–C(21)	1.425(4)
C(2)–C(3)	1.353(5)	C(21)–C(26)	1.421(4)
N(4)–C(5)	1.355(4)	C(21)–C(22)	1.423(4)
N(4)–C(9)	1.359(4)	C(22)–C(23)	1.366(4)
C(5)–C(6)	1.376(4)	C(23)–C(24)	1.401(5)
C(6)–C(7)	1.373(5)	C(24)–C(25)	1.357(5)
C(7)–C(8)	1.374(5)	C(25)–C(26)	1.417(4)
C(8)–C(9)	1.383(4)	C(26)–C(27)	1.415(4)
C(9)–C(10)	1.487(4)	C(27)–C(28)	1.366(4)
C(10)–C(19)	1.386(4)	C(28)–C(29)	1.408(4)
C(10)–C(11)	1.417(4)	C(29)–C(30)	1.478(4)
C(11)–C(12)	1.361(5)	C(30)–N(35)	1.365(4)
C(12)–C(13)	1.420(5)	C(30)–C(31)	1.389(4)
C(13)–C(18)	1.416(4)	C(31)–C(32)	1.383(5)
C(13)–C(14)	1.427(4)	C(32)–C(33)	1.366(5)
C(14)–C(15)	1.360(5)	C(33)–C(34)	1.382(5)
C(15)–C(16)	1.400(5)	C(34)–N(35)	1.345(4)
C(2)–Pd(1)–N(35)	123.92(14)	C(16)–C(17)–C(18)	121.2(3)
C(2)–Pd(1)–C(1)	37.06(14)	C(13)–C(18)–C(19)	119.5(3)
N(35)–Pd(1)–C(1)	91.01(12)	C(13)–C(18)–C(17)	117.7(3)
C(2)–Pd(1)–C(3)	36.97(14)	C(19)–C(18)–C(17)	122.8(3)
N(35)–Pd(1)–C(3)	158.50(11)	C(10)–C(19)–C(18)	119.7(3)
C(1)–Pd(1)–C(3)	67.58(13)	C(10)–C(19)–C(20)	120.6(3)
C(2)–Pd(1)–N(4)	128.39(14)	C(18)–C(19)–C(20)	119.6(3)
N(35)–Pd(1)–N(4)	105.12(9)	C(29)–C(20)–C(21)	119.5(3)
C(1)–Pd(1)–N(4)	163.82(12)	C(29)–C(20)–C(19)	118.2(3)
C(3)–Pd(1)–N(4)	96.26(11)	C(21)–C(20)–C(19)	122.2(2)
C(2)–C(1)–Pd(1)	70.9(2)	C(26)–C(21)–C(22)	118.3(3)
C(3)–C(2)–C(1)	123.2(4)	C(26)–C(21)–C(20)	119.3(3)
C(3)–C(2)–Pd(1)	72.4(2)	C(22)–C(21)–C(20)	122.5(3)
C(1)–C(2)–Pd(1)	72.1(2)	C(23)–C(22)–C(21)	120.6(3)
C(2)–C(3)–Pd(1)	70.6(2)	C(22)–C(23)–C(24)	120.8(3)
C(5)–N(4)–C(9)	117.0(3)	C(25)–C(24)–C(23)	120.1(3)
C(5)–N(4)–Pd(1)	115.9(2)	C(24)–C(25)–C(26)	120.2(3)
C(9)–N(4)–Pd(1)	124.8(2)	C(27)–C(26)–C(25)	121.6(3)
N(4)–C(5)–C(6)	123.8(3)	C(27)–C(26)–C(21)	119.4(3)
C(7)–C(6)–C(5)	118.5(3)	C(25)–C(26)–C(21)	119.0(3)
C(6)–C(7)–C(8)	118.6(3)	C(28)–C(27)–C(26)	120.5(3)
C(7)–C(8)–C(9)	120.8(3)	C(27)–C(28)–C(29)	120.7(3)
N(4)–C(9)–C(8)	121.0(3)	C(20)–C(29)–C(28)	120.5(3)
N(4)–C(9)–C(10)	119.8(3)	C(20)–C(29)–C(30)	117.8(3)
C(8)–C(9)–C(10)	119.1(3)	C(28)–C(29)–C(30)	121.5(3)
C(19)–C(10)–(11)	120.1(3)	N(35)–C(30)–C(31)	121.1(3)
C(19)–C(10)–C(0)	120.1(3)	N(35)–C(30)–C(29)	117.5(2)
C(11)–C(10)–C(9)	119.6(3)	C(31)–C(30)–C(29)	121.1(3)
C(12)–C(11)–C(10)	120.8(3)	C(32)–C(31)–C(30)	119.5(3)
C(11)–C(12)–C(13)	120.6(3)	C(33)–C(32)–C(31)	119.0(3)
C(18)–C(13)–C(12)	119.1(3)	C(32)–C(33)–C(34)	119.1(3)
C(18)–C(13)–C(14)	119.4(3)	N(35)–C(34)–C(33)	123.0(3)
C(12)–C(13)–C(14)	121.5(3)	C(34)–N(35)–C(30)	117.5(3)
C(15)–C(14)–C(13)	120.7(3)	C(34)–N(35)–Pd(1)	117.9(2)
C(14)–C(15)–C(16)	120.3(3)	C(30)–N(35)–Pd(1)	121.5(2)
C(17)–C(16)–C(15)	120.7(3)		

distinct molecules of **21** were found in the asymmetric unit although the bond lengths and angles in each are very similar and selected values for only one of the molecules are given in Table 2. The molecule crystallises as a racemic mixture in triclinic space group $P\bar{1}$. The structure of **21** consists of a cationic palladium complex containing the same chelating ligand (**6**) found in **20** with an η^3-allyl ligand also present. The co-ordination geometry around the palladium atom may be described as near square planar with respect to the outer carbon atoms of the allyl ligand and the nitrogen atoms of the dipyridylbinaphthyl ligand **6**. A triflate anion balances the charge on the metal complex. The bond length between the naphthalene rings C(19)–C(20) 1.501(4) is nearly identical to that found in **20**. The torsion angle C(18)–C(19)–C(20)–C(21) between the naphthalene rings is also similar (−104.5°) while the torsion angles between the pyridyl groups and naphthalene

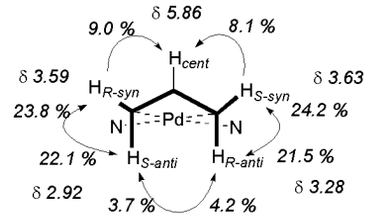

pro-S, *pro*-R labeling scheme for allyl protons
(δ-values only apply to (+)-**21** bearing M-helicity (aR) (+)-**6**)
and intra-allyl NOE contacts

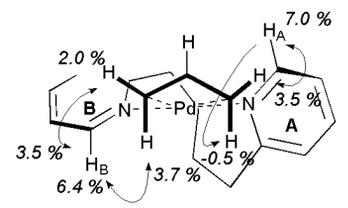

allyl-pyridyl NOE contacts
(H_A and H_B degenerate at NMR time scale)

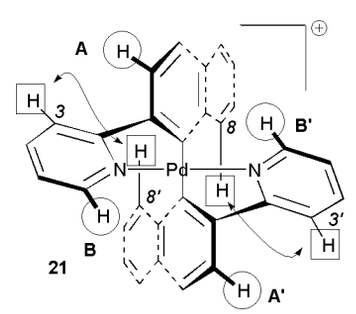

Protons in ligand 6
Circled: broadened due to A/A' and B/B'
δ-exchange at NMR time scale
Squared: NOE contacts

Fig. 3 Upper: nomenclature for allyl protons in complex **21** together with chemical shifts and identification by intra-allyl and inter-allyl ligand NOE difference spectroscopy. Lower: selected features of ^{1}H NMR of **21**.

rings are found to be a little smaller than the corresponding angles in complex **20** [N(4)–C(9)–C(10)–C(19) 63.9 and N(35)–C(30)–C(29)–C(20) 61.9°]. This is presumably a reflection of the square-planar co-ordination requirements of the 16-electron palladium centre.

Palladium allyl complexes are often fluxional in solution and study of the stereodynamic mechanism(s), which can be diverse and simultaneous, can provide useful information relevant to their involvement in catalysis.[16] In η^3-allyl complexes the ligand presents a symmetrical face to the metal and the five protons may be divided into three groups: central (1 H), *syn* (2 H, one *pro-S*, the other *pro-R*) and *anti* (2 H, again *pro-S* and *pro-R*), see Fig. 3. In the case of complex **21**, although both ligand (**6**) donors are pyridyl nitrogen, the C_2-symmetric chirality of the ligand in the square plane results in all five allyl protons being magnetically unique, providing stereodynamic processes do not equilibrate them faster than the NMR timescale. By performing COSY, direct CH correlation and NOE difference experiments (NOED), all ligand (**6**) and η^3-allyl ^{1}H NMR (CD_2Cl_2) signals of **21** could unambiguously be assigned (see upper part of Fig. 3).

Allyl ligand proximity evidenced by NOED allows distinction of *pro-*S_{anti} and *pro-R*,S_{syn} (all have positive enhancements on irradiation of the two time-average degenerate protons H_A/

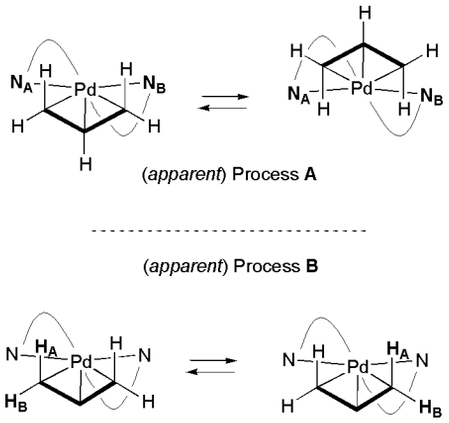

Fig. 4 Schematic representations (a sigmoidal curve is used to represent ligand **6**) of the two basic (*apparent*) stereodynamic processes (**A** and **B**) occurring in complex **21**.

H_B at position six of the pyridyl rings, see middle part of Fig. 3) from *pro-*R_{anti} which displays a *negative* enhancement on irradiation of the same pyridyl protons.‡‡ The NOED results are fully consistent with the crystal structure (Fig. 2, upper structure) where the proximity of *pro-*S_{anti} and *pro-*R,S_{syn} to the pyridyl proton on C(5) and the near linearity of the C(34)–H/*pro-*S_{syn}/*pro-*R_{anti} three spin system are self evident. Furthermore, NOE contact is observed between degenerate pyridyl C(3,3′)–H and naphthyl C(8,8′)–H (bottom part of Fig. 3). These NOE contacts must occur between (and not within) the two 'halves' of the ligand **6** (*i.e.* C(8)–H with C(22)–H and C(31)–H with C(17)–H in the lower structure in Fig. 2). This establishes that a wide bite angle is maintained in solution since the proximity of the pair of pyridyl C(3,3′)–H and naphthyl C(8,8′)–H protons is dependent on both a large deviation from coplanarity of (a) the naphthyl rings by rotation about the atropisomeric axis and (b) the pyridylnaphthyl rings by rotation about the naphthyl C(2,2′)–pyridyl C(2,2′) bonds. These results suggest that the co-ordination mode of **6** in **21** as determined by X-ray diffraction is maintained, to a reasonable degree, in solution.

There were two curious features about the ^{1}H NMR spectrum (CD_2Cl_2, 300 and 500 MHz) of complex **21** ([Pd(η^3-C_3H_5)((±)-**6**)][OTf]). First, the allyl unit displayed five multiplets, each with sharp lines ($\omega_{1/2} \leq 1$ Hz). Secondly, the ligand (**6**) displayed only 10 multiplet signals (each 2 H) and each was sharp, except for those assigned as arising from pyridyl C(6)–H and naphthyl C(3)–H, which are both a pair of degenerate 2 H. These two protons project over the palladium co-ordination sphere (see circled protons at bottom of Fig. 3) and are therefore by far the most sensitive to the disposition of the allyl unit. The 2-D PNOSY (phase enhanced nuclear Overhauser effect spectroscopy) spectrum of complex **21** (500 MHz, CD_2Cl_2, 25 °C, N_2-saturated) demonstrated that there was site exchange (positive phase cross-peaks) between the two *anti* and between the two *syn* protons on the allyl unit. There were no exchange cross-peaks between *syn* and *anti* protons, although there were of course NOE cross-peaks (negative phase) between *pro-*S_{anti} and *pro-*R_{syn} and between *pro-*R_{anti} and *pro-*S_{syn}.

Having assigned identities to the all of the ligand (**6**) protons and the allyl protons, interpretation of the stereodynamic processes becomes possible. There are two processes that are apparent, Fig. 4. The first process (**A** in Fig. 4) is just faster than the NMR timescale and results in a time-average C_2-symmetric environment around the ligand **6**, that is ten multiplets are observed (each integrating for 2 H) rather than the twenty that would be observed if process **A** was slow or not present. The second process (**B**) involves *apparent* epimerisation of the Pd–π-allyl face, that is there is an apparent mutual exchange of *pro-*S_{anti} with *pro-*R_{anti} and of *pro-*R_{syn} with *pro-*S_{syn}. However, it should be noted that the pseudoenantiomeric protons *pro-R*/S_{anti} and *pro-R*/S_{syn} are only magnetically distinguishable in the presence of the C_2-symmetric chiral ligand **6**. Since the π-allyl ligand has a mirror plane of symmetry, the two halves of **6** are inequivalent with respect to a static Pd–allyl fragment. Therefore, process **A** must effect 180° rotation of either (i) ligand **6** about the Pd(η^3-allyl) fragment or (ii) the allyl unit about the [Pd(**6**)] fragment. The absence of *syn–anti* exchange in the PNOSY spectrum (spin-mixing time, τ_m, was 300 ms) indicates that the allyl fragment remains bound to Pd in a planar mode (*i.e.* η^3 or η^2) throughout process **B** and also that mode (ii) of process **A** (which would occur *via* an η^1-allyl intermediate) is not dominant.

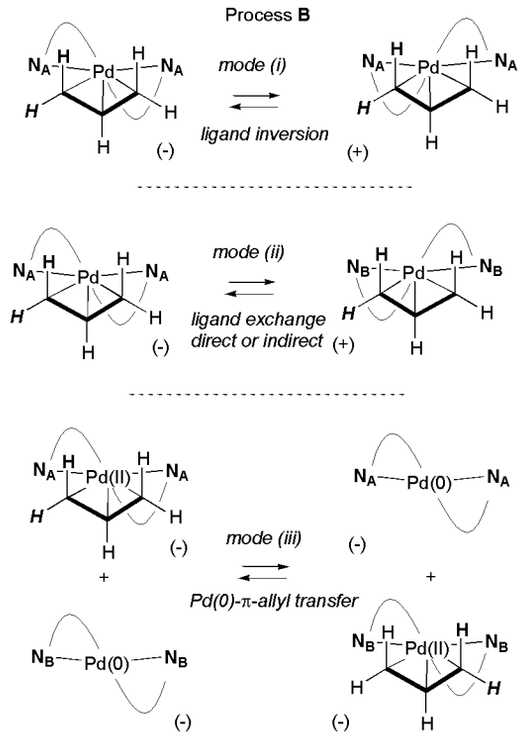

Fig. 5 Mechanisms (modes i–iii) considered and tested for stereodynamic process **B** occurring in complex **21**. Note that mode (i) is unimolecular whilst (ii) and (iii) are bimolecular. The last two are distinguishable by the requirement of enantiomerically opposite ligand for mode (ii) and enantiomerically identical ligand for (iii). Thus, in enantiomerically pure complex **21**, mode (ii) is unavailable whilst the rate of (iii) would be increased relative to that of the racemate.

For process **B** the *apparent* epimerisation of the Pd–π-allyl face could arise by at least three mechanisms (see Fig. 5): (i) *intra*molecular enantiomerisation of the ligand **6**; (ii) *inter*molecular exchange (direct or indirect) of **6** between two complexes of *opposite* configuration or (iii) *inter*molecular transfer of the Pd–π-allyl, with inversion, to another **6**–Pd unit of the *same* configuration.[17] This latter process may occur if a catalytic quantity of **6**–Pd^0 is generated by attack of trace nucleophile on the allyl of [Pd(η^3-C_3H_5)(**6**)][OTf].

Mode (i) in process **B** was readily eliminated from consideration by the observation that the optical rotation of [Pd(η^3-C_3H_5)((−)-**6**)][OTf] in CH_2Cl_2 was constant over a period of hours. Furthermore, treatment of the complex with 1 equivalent dppf (to generate [Pd(dppf)(η^3-C_3H_5)][OTf]) allowed recovery of (−)-**6**, after silica gel chromatography, in 74% yield and >96% ee. We are thus left with two possible modes (ii and iii) for process **B**.

When 5 mol% free compound (±)-**6** was added to the NMR (CD_2Cl_2) sample of complex **21** [Pd(η^3-C_3H_5)((±)-**6**)][OTf] the

‡‡ It should be noted that the stereochemical notation *pro-S* and *pro-R* applies to complex (+)-**21** bearing *M*-helicity (*aR*) (+)-**6** and assignments are reversed in (−)-**21**.

1-D spectrum appeared identical with that of pure **21**, with no trace of the added **6**. Indeed, the free **6** was so extensively broadened that only the peaks arising from pyridyl protons C(3)–H and C(6)–H were evident, and then only as slight bumps in the baseline. The PNOSY spectrum showed the presence of positive phase intermolecular exchange cross-peaks in the aromatic region. These were identified (by reference to the 1-D spectrum of pure **6**) as those arising from exchange between free **6** and Pd-complexed **6**. Indeed, 8 out of the 10 degenerate pairs of protons of free **6** were directly correlated with the complex. The remaining two (naphthyl C(3,3′)–H and C(4,4′)–H) could not be correlated since they have near-identical chemical shifts for the "free" ligand and complex **21**. These exchange cross-peaks demonstrate that the "free" ligand is in exchange with **21**, but not whether this is a direct exchange or involved in process **A** or **B**. However, a 1.5-fold increased intensity of the *anti–anti* and *syn–syn* exchange cross-peaks (relative to those observed in the absence of added free **6**) indicates that free **6** accelerates process **B**.

A second important piece of evidence came from the PNOSY spectrum of the *enantiomerically pure* complex (−)-**21** {[Pd(η^3-C_3H_5)((−)-**6**)][OTf]}. This was almost identical to that of the *racemate* (±)-**21**, except that the exchange cross-peaks (positive phase) between *anti–anti* and between *syn–syn* allyl protons had been replaced by weak negative phase (NOE) cross-peaks. To confirm that *anti–anti* exchange was indeed absent, the excess of spin population of the upfield *anti*-allyl proton (δ 2.92) of (−)-**21** (1-D ^{1}H NMR, 500 MHz) was selectively inverted by a DANTE pulse-train,[18] with variable delay time (τ) (0–4500 ms) before a 'read-pulse' (π/2) was applied. With increasing τ, an NOE was observed to develop then decay at both the geminal *syn* proton (δ 3.59) and the other *anti* proton (δ 3.28), the former having a higher build-up rate, consistent with its greater proximity. Importantly, at lower values of τ, before NOE build-up, there was no attenuation of the intensity of the *anti* proton at δ 3.28 and therefore no evidence for chemical exchange between the two *anti* protons. Thus the exchange process **B** in **21** must be dependent upon the availability of enantiomeric ligand **6** and this suggests mode (ii), *i.e.* an intermolecular exchange (direct or indirect) of (−)-**6** with (+)-**6** between complexes (+/−)-**21**. A ligand exchange process was found by Faller *et al.* to be the dominant mode of *apparent* epimerisation of the Pd–π-allyl face in the complex [Pd(AMBA)(Cl)(η^3-C_3H_5)] (AMBA = α-methylbenzylamine).[19] In the latter case exchange proceeded *via* equilibrium of [Pd(AMBA)(Cl)(η^3-C_3H_5)] with free AMBA and the chloro-dimer [Pd_2Cl_2(η^3-C_3H_5)$_2$] which was clearly observable in the ^{1}H NMR spectrum at low temperatures. However, in the current case a close inspection of the PNOSY spectrum of (±)-**21** revealed *anti–anti* and *syn–syn* exchange cross-peaks between the ^{13}C satellites of the *anti*- and *syn*-allyl ^{1}H signals of **21** and therefore there is no evidence for any other Pd–allyl species, above *ca.* 0.5% abundance, involved in exchange at the NMR timescale with **21**.[20]

To unify the mechanisms of the stereodynamic processes we may consider the following. The line broadening of pyridyl C(6,6′)–H and naphthyl C(3,3′)–H observed in the *enantiomerically pure* complex (−)-**21** is identical with that observed in the *racemate* (±)-**21** and both are concentration independent; this rules out attack of free **6** on **21** and subsequent Berry pseudorotation in a five-co-ordinate complex of type [Pd(η^3-C_3H_5)(**6**)$_2$][OTf] as being the primary mode for exchange process **A**. This then suggests that **A** is unimolecular and involves equilibrium with a species in which **6** functions as a monodentate ligand. N–Pd rotation in this species followed by reco-ordination of **6** in bidentate mode would result in a time-average C_2-symmetrical environment about the ligand **6**. It is reasonable to assume that the species involving monodentate co-ordination of **6** would be much more reactive towards free **6** than complex **21** (bidentate **6**) since the Pd is co-ordinatively

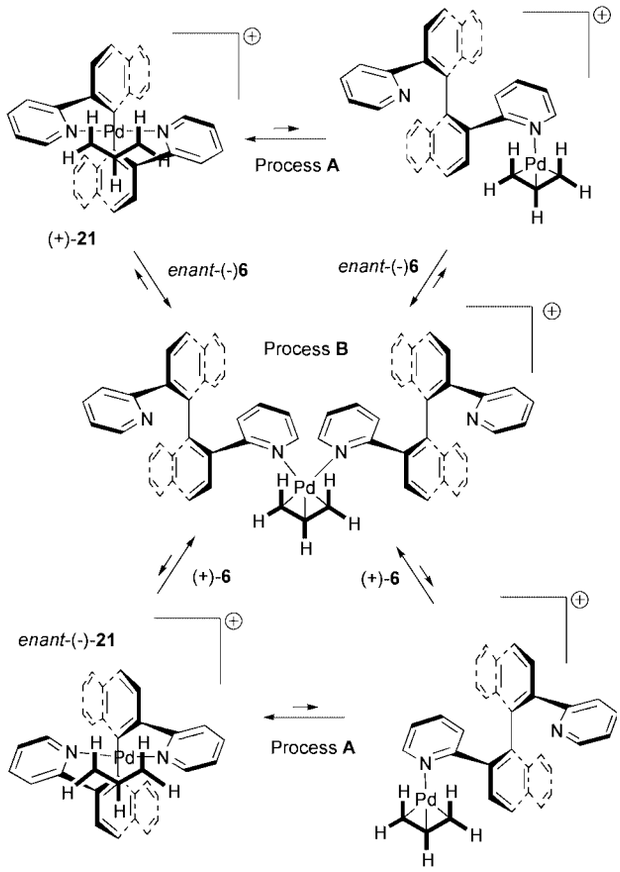

Scheme 3 A unified mechanistic sequence to account for stereodynamic processes **A** and **B** observed by ^{1}H NMR in complex (±)-**21**. Only **A** is observed with enantiomerically pure compex **21**.

unsaturated (or loosely complexed by solvent) and also since the steric encumbrance of **6** is reduced in monodentate mode. However, this does not rule out a direct attack of free **6** on **21** at a rate slower than process **A**. In any event, either mode of attack of enantiomeric ligand *enant*-**6** (direct or indirect) on **21** would give rise to a species that could lose ligand **6** to give *enant*-**21** and thereby effect process **B**. A unified mechanism for process **A** and the major mode of process **B** is presented in Scheme 3.

It therefore appears that although compound **6** can function as a bidentate ligand towards a π-allyl palladium cationic species, the co-ordination is kinetically labile and there is fairly rapid equilibrium with an energetically less favourable, but accessible, species in which **6** functions as a monodentate ligand. This equilibrium may well decrease the efficacy with which there may be chiral relay from the atropisomeric axis to reactions occurring in the palladium-co-ordination sphere. We will report on the application of **6** to asymmetric catalysis in due course.

Conclusion

We have prepared enantiomerically pure atropisomeric ligand **6** in five steps from commercially available 2-naphthol. Despite many different attempts we were unable to introduce two pyridyl groups onto a binaphthyl skeleton (strategy **A**, Scheme 1) and therefore resorted to a homocoupling strategy (**B**, Scheme 1). This Ni-catalysed dehalogenative process is less susceptible to steric hindrance induced by groups in the 2 position of the homocoupling partners than analogous reactions involving triflates.[21] The absolute stereochemistry (axial chirality *aR*/*aS* or helicity *P*/*M*) of the two enantiomers of **6** was assigned by circular dichroism spectroscopy. The ligand is stable (chemically and chiroptically), easily handled, and read-

Table 3 Crystallographic data for complexes **20** and **21**

	20	**21**
Crystallised from	Ethyl acetate	CH_2Cl_2–Et_2O
Formula	$C_{30}H_{20}Cl_2N_2Zn$	$C_{34}H_{25}F_3N_2O_3PdS$
M	544.8	705.0
Crystal system	Monoclinic	Triclinic
Space group	$P2_1/c$	$P\bar{1}$
a/Å	18.672(2)	10.766(3)
b/Å	9.045(1)	15.359(4)
c/Å	15.919(2)	18.607(4)
α/°		89.95(2)
β/°	110.510(9)	80.42(2)
γ/°		85.26(2)
U/Å^3	2518.3(5)	3023.1(13)
T/K	173	173
Z	4	4
μ/mm^{-1}	1.21	0.74
Reflections measured	25226	25936
Unique reflections	5741	10584
R_{int}	0.025	0.029
Observed reflections	4882	8225
$wR2$ (all data, on F^2)	0.061	0.084
$R1$ [data with $F^2 > 2\sigma(F^2)$]	0.022	0.033
Extinction parameter, x	0.0026(2)	0.0010(2)

ily prepared. We have studied the co-ordination chemistry of **6** and shown that it may function as a bidentate ligand to both Zn^{II} (to form complex **20**) and to Pd^{II} (to form complex **21**). These complexes are isolable, stable and fully characterised (including X-ray crystallography). The stereodynamics of *racemic* complex **21** ([Pd(η^3-C_3H_5)(**6**)][OTf]) have been studied by NMR. There are two distinct stereodynamic processes, one of which results in a time-average C_2-symmetric environment about the ligand and one of which effects *apparent* (but not genuine) interconversion of the faces of the π-allyl ligand. It is suggested that Pd–N deco-ordination followed by Pd–N rotation translation (the 'Bäckvall mechanism'[22]) is responsible for the first process, whilst enantiomeric ligand exchange is responsible for the latter. Chiral ligands for asymmetric allylic alkylation are becoming ubiquitous and there are a growing number of reported studies of the structure and stereodynamics of the catalysts. However, in nearly all cases only the enantiomerically pure ligands have been employed and stereodynamic information from NMR may have been missed.

Experimental

General

Solvents and reagents were purified by standard procedures. Anhydrous solvents were purchased from Fluka or Aldrich and used as received. When appropriate, reactions were performed under argon using standard Schlenk techniques. NMR spectra: JEOL Alpha 500, Delta 400, Lambda 300 and Delta 270; chemical shifts (ppm) are referenced to TMS (δ 0.00) or internally referenced to the lock signal of the deuteriated solvent used. Mass spectra: Micromass Autospec. IR spectra: Perkin-Elmer 1600 FTIR, absorptions are reported as strong (s), medium (m) or weak (w). Flash column chromatography: Merck silica gel 60 eluting with a constant gravity head of *ca.* 15 cm solvent. TLC: 0.25 mm, Merck silica gel 60 F254 visualised at 254 nm.

X-Ray crystallography

Crystallographic data for crystals of **20** and **21** are presented in Table 3. Measurements were made at −100 °C on a Bruker SMART CCD area-detector diffractometer with Mo-Kα radiation ($\lambda = 0.71073$ Å).[23] Intensities were integrated[24] from several series of exposures, each exposure covering 0.3° in ω, and the total data set being a sphere in each case. Absorption corrections were applied based on multiple and symmetry equivalent measurements.[25] The structure was solved by Patterson synthesis and refined by least squares on weighted F^2 values for all reflections (see Table 3).

CCDC reference number 186/1922.

See http://www.rsc.org/suppdata/dt/b0/b000651n/ for crystallographic files in .cif format.

Dynamic NMR spectroscopy

PNOSY spectra were acquired and processed on a JEOL Alpha 500 instrument operating at 500 MHz (^{1}H). Spectra of complex **21** (10 mg) were recorded in degassed, nitrogen-saturated CD_2Cl_2 (0.74 ml) at 24.6 °C (± 0.6 °C) without spinning. 32 scans were acquired per column, spin-mixing time, τ_m, was 300 ms. Data were acquired with 1024 × 512 digitisation and zero-filled to 1024 × 1024 before application of a Gaussian window. After FT-FT, phasing was adjusted by the States method and then drift and baseline corrections were applied. Spectra were plotted with colour-coded contours to indicate amplitude and phase.

Preparation of ligand and complexes

1-Chloro-2-trifluoromethylsulfonyloxynaphthalene 18. Trifluoromethanesulfonic anhydride (20.9 cm^3, 0.124 mol) was slowly added to a solution of 1-chloro-2-naphthol (20.0 g, 0.112 mol) in dry pyridine (60 cm^3) at 0 °C. The reaction mixture was stirred at room temperature for 16 hours. When the reaction was shown to be complete by TLC water (200 cm^3) was added. The product was extracted with dichloromethane (2 × 200 cm^3) and the combined organic layers were washed with water (200 cm^3), 10% HCl(aq) (2 × 200 cm^3), saturated brine (100 cm^3), dried over $MgSO_4$ and concentrated under reduced pressure. The crude orange oil was filtered through a pad of silica using ethyl acetate as the eluent. The filtrate was concentrated under reduced pressure to give white crystals of the triflate **18** (33.10 g, 95%), mp 34 °C; $\tilde{\nu}_{max}$/cm^{-1} (NaCl) 3056w, 2922m, 1589m, 1500m, 1422s, 1361m, 1322m, 1217s, 1139s, 994s, 939s, 828s and 606s (Nujol); δ_H (300 MHz; solvent $CDCl_3$; standard $SiMe_4$) 7.45 (1 H, d, J 9.2, C^3–H), 7.61 (1 H, ddd, J 1.3 and 6.9 and 7.9, C^6–H), 7.69 (1 H, ddd, J 1.5 and 6.9 and 8.3, C^7–H), 7.85 (1 H, d, J 9.2, C^4–H), 7.89 (1 H, dd, J 1.1 and 7.9, C^5–H) and 8.30 (1 H, d, J 8.3 Hz, C^8–H); δ_C (75 MHz; solvent $CDCl_3$; standard $SiMe_4$) 118.7 (q, $^1J_{CF} = 1275$ Hz, CF_3), 119.9 (C^3), 124.5 (C^{10}), 124.9 (C^8), 127.8 (C^6), 128.3 (C^5), 128.5 (C^7), 128.8 (C^4), 131.3 (C^9), 133.0 (C^1) and 143.3 (C^2); δ_F (283 MHz; solvent $CDCl_3$) −73.4 (s, CF_3); *m*/*z* (EI) 310 (M^+, 12%), 177 ($M - OSO_2CF_3$, 22) and 149 (49).

1-Chloro-2-(pyridin-2-yl)naphthalene 19. n-Butyllithium (0.53 cm^3, 1.32 mmol, 2.5 M in hexanes) was added dropwise to a solution of 2-bromopyridine (0.13 cm^3, 1.29 mmol) in dry tetrahydrofuran (10 cm^3) at −78 °C, under a blanket of argon, and the reaction stirred for one hour. Zinc(II) chloride (180 mg, 1.32 mmol) was added as a solid and the reaction allowed to warm to room temperature, whereupon the mixture changed from yellow to pale pink. [1,3-Bis(diphenylphosphino)propane] palladium dichloride (19 mg, 0.032 mmol) was added followed by a solution of 1-chloro-2-trifluoromethylsulfonyloxynaphthalene **18** (200 mg, 0.64 mmol) in dry tetrahydrofuran (2 cm^3). The reaction was then heated at 60 °C for 16 hours until complete by TLC when water (20 cm^3) was added. The organic layer was separated and the aqueous layer extracted with CH_2Cl_2 (2 × 20 cm^3). The combined organic layers were washed with water (20 cm^3), dried over $MgSO_4$, and concentrated under reduced pressure. The yellow solid was purified by column chromatography (20% ethyl acetate in hexane) to give white crystals of *1-chloro-2-(pyridin-2-yl)naphthalene* **19** (125 mg, 82%), mp 85 °C (Found: C, 75.24; H, 4.05; N, 5.70. $C_{15}H_{10}ClN$ requires C,

75.16; H, 4.20; N, 5.84%); $\tilde{\nu}_{max}/cm^{-1}$ (KBr) 1583s, 1474s, 1431s, 1327m, 1246m, 1147w, 1088w, 1044w, 973m, 864w, 821s, 782s, 767s, 744s, 663w and 543m; δ_H (300 MHz; solvent $CDCl_3$; standard $SiMe_4$) 7.32 (1 H, ddd, *J* 2.9 and 5.0 and 5.9, C_{pyr}^5–H), 7.57 (1 H, ddd, *J* 1.0 and 6.9 and 8.0, C^6–H), 7.64 (1 H, ddd, *J* 1.0 and 6.9 and 8.4, C^7–H), 7.69 (1 H, d, *J* 8.4, C^3–H), 7.75 (1 H, m, C_{pyr}^4–H), 7.81 (1 H, m, C_{pyr}^3–H), 7.86 (1 H, d, *J* 8.4, C^4–H), 7.90 (1 H, ddd, *J* 0.7, 1.0 and 8.0, C^5–H), 8.42 (1 H, ddd, *J* 0.7, 1.0 and 8.4 Hz, C^8–H) and 8.77 (1 H, ddd, *J* 1.1, 1.1 and 5.0 Hz, C_{pyr}^6–H); δ_C (75 MHz, solvent $CDCl_3$, standard $SiMe_4$) 122.4 (C_{pyr}^5), 125.1 (C^8), 125.6 (C_{pyr}^4), 127.0 (C^6), 127.1 (C^4), 127.4 (C^7), 128.0 (C^3), 128.1 (C^5), 129.6 (C^{10}), 131.1 (C^9), 134.2 (C^1), 135.9 (C_{pyr}^3), 136.4 (C^2), 149.5 (C_{pyr}^6) and 157.5 (C_{pyr}^2); *m/z* (EI) 241 ($M^+(^{37}Cl)$, 33%), 239 ($M^+(^{35}Cl)$, 100) and 204 (M − Cl, 100).

Racemic 2,2′-bis(pyridin-2-yl)-1,1′-binaphthalene 6. A mixture of bis(triphenylphosphine)nickel dichloride (4.78 g, 7.30 mmol), zinc (1.43 g, 21.9 mmol) and tetraethylammonium iodide (3.76 g, 14.6 mmol) was stirred in dry tetrahydrofuran (150 cm^3), under argon, until it had turned from green to deep red. A solution of 1-chloro-2-(pyridin-2-yl)naphthalene **19** (3.50 g, 14.6 mmol) in dry tetrahydrofuran (40 cm^3) was added and stirred at room temperature until the substrate could not be detected by TLC (ethyl acetate). Water (100 cm^3) was added and filtered through a pad of Celite®. The solids were added to the organic layers and this mixture was extracted with 10% aqueous HCl (2 × 100 cm^3). The combined aqueous layers were taken to pH 13 with sodium hydroxide pellets to give a white precipitate and extracted with dichloromethane (2 × 100 cm^3). The combined organic layers were dried over $MgSO_4$ and concentrated under reduced pressure until approximately 10 cm^3 was left. An equal volume of *tert*-butyl methyl ether was added and the mixture extracted with 10% aqueous HCl (3 × 50 cm^3). The combined aqueous layers were taken to pH 13 by addition of sodium hydroxide pellets, giving a white precipitate. The product was extracted with dichloromethane (3 × 100 cm^3) and the combined organic layers were dried over $MgSO_4$ and concentrated under reduced pressure. The resulting orange oil was purified by column chromatography (ethyl acetate) to give white crystals of *2,2′-bis(pyridin-2-yl)-1,1′-binaphthalene* **6** (2.06 g, 69%), mp 163–165 °C (Found: C, 87.90; H, 4.67; N, 6.71. $C_{15}H_{10}N$ requires C, 88.21; H, 4.93; N, 6.86%). $\tilde{\nu}_{max}/cm^{-1}$ (KBr) 1583w, 1472w, 1433m, 1183s, 1117s, 750m, 720s, 697s and 547s. δ_H (300 MHz; solvent C_6D_6) 6.35 (2 H, ddd, *J* 1.1 and 4.8 and 7.7, C_{pyr}^5–H and $C_{pyr}^{5'}$–H), 6.61 (2 H, ddd, *J* 1.4 and 7.7 and 7.8, C_{pyr}^4–H and $C_{pyr}^{4'}$–H), 6.95 (2 H, ddd, *J* 1.1 and 1.4 and 7.8, C_{pyr}^3–H and $C_{pyr}^{3'}$–H), 6.97 (2 H, ddd, *J* 1.3 and 6.9 and 8.3, C^6–H and $C^{6'}$–H), 7.15 (2 H, ddd, *J* 1.1 and 6.9 and 8.2, C^7–H and $C^{7'}$–H), 7.56 (2 H, dd, *J* 1.1 and 8.3, C^5–H and $C^{5'}$–H), 7.67 (2 H, d, *J* 8.2, C^8–H and $C^{8'}$–H), 7.79 (2 H, d, *J* 8.8, C^4–H and $C^{4'}$–H), 8.10 (2 H, d, *J* 8.8, C^3–H and $C^{3'}$–H) and 8.28 (2 H, ddd, *J* 1.0, 1.8 and 4.8 Hz, C_{pyr}^6–H and $C_{pyr}^{6'}$–H); δ_C (75 MHz, solvent C_6D_6) 121.6 (C_{pyr}^5 and $C_{pyr}^{5'}$), 124.4 (C_{pyr}^3 and $C_{pyr}^{3'}$), 126.8 (C^7 and $C^{7'}$), 127.2 (C^6 and $C^{6'}$), 127.8 (C^5 and $C^{5'}$), 128.8 (C^8 and $C^{8'}$), 129.2 (C^3 and $C^{3'}$), 134.1 (C^{10} and $C^{10'}$), 134.4 (C^9 and $C^{9'}$), 135.2 (C_{pyr}^4 and $C_{pyr}^{4'}$), 135.6 (C^1 and $C^{1'}$), 140.0 (C^2 and $C^{2'}$), 149.5 (C_{pyr}^6 and $C_{pyr}^{6'}$) and 158.3 (C_{pyr}^2 and $C_{pyr}^{2'}$); *m/z* (EI) 408 (M^+, 77%), 330 ($M - C_6H_5N$, 100) and 204 ($M - C_{15}H_{10}N$, 11). HRMS(EI): found *m/z* 408.1617, $C_{30}H_{20}N_2$ requires 408.1626.

Resolution of ***6***. A solution of L-tartaric acid (368 mg, 2.45 mmol) in acetone (20 cm^3) was added to a solution of 2,2′-bis(pyridin-2-yl)-1,1′-binaphthalene **6** (500 mg, 1.23 mmol) in dichloromethane (10 cm^3). The solvent was removed under reduced pressure to give a gummy white solid. The solid was refluxed in ethyl acetate until no more dissolved. The solution was decanted and left at −4 °C for 16 h. The resulting white gel was separated by filtration (sinter plate) and then collected by dissolution in acetone. Both the solutions (filtrate and acetone extract) were concentrated under reduced pressure. The resulting solids were dissolved in dichloromethane (20 cm^3) and washed with 1 M NaOH. The organic layer was dried over $MgSO_4$ and concentrated under reduced pressure to give 147 mg of compound (−)-**6** (from the gel) and 193 mg of (+)-**6** (from the filtrate). ^1H NMR studies in C_6D_6 after addition of (+)-Eu(hfc)$_3$ (0.4 equivalent) showed (+)-**6** to 77% ee and (−)-**6** to be 75% ee. Both samples were enriched by repeating the above procedure with the appropriate enantiomer of tartaric acid until the minor enantiomer of **6** could no longer be detected by NMR in the presence of (+)-Eu(hfc)$_3$ and the sample was judged >96% ee, mp 104 °C. (−)-**6**: $[\alpha]_D$ (*c* = 1.00, CH_2Cl_2, 22 °C) = −20.81 deg cm^3 g^{-1} dm^{-1} [a six point plot of $[\alpha]_D$ (at *c* = 1.00) *versus* ee (0–100%) was linear (r^2 = 0.999)]. All other spectral data (NMR, IR, MS) identical with racemate.

[2,2′-Bis(pyridin-2-yl)-1,1′-binaphthalene]dichlorozinc(II) (±)-20. A solution of zinc dichloride (14.4 mg, 0.105 mmol) in acetonitrile (2 cm^3) was added to a solution of 2,2′-bis(pyridin-2-yl)-1,1′-binaphthalene **6** (43.0 mg, 0.105 mmol) in acetonitrile (2 cm^3). The solvent was removed under reduced pressure and the white solid heated in ethyl acetate (5 cm^3). On cooling white crystals appeared and these were separated from the mother liquor by decantation to give $[ZnCl_2(C_{30}H_{20}N_2)]$ **20** (40 mg, 70%), mp ≥300 °C (darkens) (Found: C, 65.85; H, 4.01; N, 5.14. $C_{30}H_{20}Cl_2N_2Zn$ requires: C, 66.14; H, 3.70; N, 5.14%); $\tilde{\nu}_{max}/cm^{-1}$ 1603s, 1565m, 1488s, 1433m, 1283m, 1162w, 1054m, 1026m, 826s, 798s, 775m, 751m, 715w, 646w, 559w, 532w and 419w; δ_H (300 MHz; solvent CD_3CN) 7.09 (2 H, ddd, *J* 0.6 and 1.0 and 8.2, C^5–H and $C^{5'}$–H), 7.17 (2 H, ddd, *J* 1.0 and 6.6 and 8.2, C^6–H and $C^{6'}$–H), 7.19 (2 H, ddd, *J* 1.6 and 5.5 and 7.9, C_{pyr}^5 and $C_{pyr}^{5'}$–H), 7.38 (2 H, ddd, *J* 1.3, 6.6 and 8.0, C^7–H and $C^{7'}$–H), 7.68 (2 H, d, *J* 8.4, C^3–H and $C^{3'}$–H), 7.75 (2 H, ddd, *J* 0.9, 1.6 and 7.9, C_{pyr}^3–H and $C_{pyr}^{3'}$–H), 7.82 (2 H, ddd, *J* 1.7, 7.9 and 7.9, C_{pyr}^4–H and $C_{pyr}^{4'}$–H), 7.84 (2 H, d, *J* 8.0, C^8–H and $C^{8'}$–H), 8.03 (2 H, d, *J* 8.4, C^4–H and $C^{4'}$–H) and 8.43 (2 H, ddd, *J* 0.9, 1.7 and 5.5 Hz, C_{pyr}^6–H and $C_{pyr}^{6'}$–H); δ_C (75 MHz; solvent CD_3CN) 124.0 (C_{pyr}^5 and $C_{pyr}^{5'}$), 127.0 (C^5 and $C^{5'}$), 127.5 (C^3 and $C^{3'}$), 127.6 (C^6 and $C^{6'}$), 127.9 (C^7 and $C^{7'}$), 128.8 (C^8 and C8′), 128.9 (C_{pyr}^3 and $C_{pyr}^{3'}$), 129.8 (C^4 and $C^{4'}$), 131.1 (quaternary C), 134.3 (quaternary C), 137.5 (quaternary C), 141.1 (C_{pyr}^4 and $C_{pyr}^{4'}$), 148.0 (C_{pyr}^6 and $C_{pyr}^{6'}$) and 160.2 (quaternary C). *m/z* (FAB$^+$) 567 (M + Na, 5.6%) [isotope cluster 574–565: obs. (calc.) 0.4 (0.3), 0.6 (0.6), 1.7 (1.7), 1.6 (1.6), 4.2 (4.2), 2.1 (2.3), 5.6 (5.6), 1.4 (1.5), 4.4 (4.4)], 507 (M − Cl, 100) [isotope cluster 515–507: obs. (calc.) 1 (1), 5 (5), 18 (18), 23 (24), 63 (65), 42 (40), 95 (95), 38 (35), 100 (100)], 431 (M − ZnCl_2 + Na, 5), 409 (M − $ZnCl_2$ + H, 57), 408 (M − $ZnCl_2$, 57), 330 (18) and 279 (8).

(η³-Allyl)[2,2′-bis(pyridin-2-yl)-1,1′-binaphthalene]-palladium(II) trifluoromethanesulfonate 21. A solution of 2,2′-bis(pyridin-2-yl)-1,1′-binaphthalene **6** (50 mg, 0.12 mmol) in dichloromethane (2 cm^3) was added to a solution of $[Pd(MeCN)_2(C_3H_5)][OSO_2CF_3]$ (46.4 mg, 0.12 mmol) in dichloromethane (2 cm^3). After five minutes the solution was filtered through a pad of Celite® and the solvent removed under reduced pressure. The resulting yellow solid was dissolved in dichloromethane (1 cm^3) and layered with diethyl ether. After 24 hours the solvent was decanted to leave yellow crystals of $[Pd(C_3H_5)(C_{30}H_{20}N_2)]OSO_2CF_3$ **21** (61 mg, 71%), mp 196 °C (Found: C, 58.29; H, 3.25; N, 3.91. $C_{34}H_{25}F_3N_2O_3PdS$ requires: C, 57.92; H, 3.57; N, 3.97%); $\tilde{\nu}_{max}/cm^{-1}$ 1736w, 1562m, 1439m, 1228w, 1018w, 894m, 863m, 813s, 760s, 695, 621m and 476s; δ_H (300 MHz; solvent CD_2Cl_2) [NB notation of allyl proton stereochemistry is relative and not absolute and refers to the complex bearing the (+)-enantiomer of **6** (*M* or *aR* helicity)] 2.92 (1 H, d, *J* 12.1, allyl CH-*pro-*S_{anti}), 3.28 (1 H, d, *J* 12.5, allyl CH-*pro-*R_{anti}), 3.59 (1 H, dd, *J* 2.3 and 7.0, allyl CH-*pro-*R_{syn}),

3.63 (1 H, dd, *J* 2.3 and 7.0, allyl CH-*pro*-S_{syn}), 5.86 (1 H, dddd, *J* 7.0, 7.0, 12.1 and 12.5, CH_2CH), 6.86 (2 H, ddd, *J* 1.8, 5.7 and 7.5, C_{pyr}^{5}–H and $C_{pyr}^{5'}$–H), 7.01 (2 H, dd, *J* 1.3 and 8.4, C^{8}–H and $C^{8'}$–H), 7.17 (2 H, ddd, *J* 1.3, 6.8 and 8.3, C^{7}–H and $C^{7'}$–H), 7.39 (2 H, ddd, *J* 1.1, 6.8 and 8.2, C^{6}–H and $C^{6'}$–H), 7.46 (2 H, ddd, *J* 0.7, 1.8 and 7.8, C_{pyr}^{3}–H and $C_{pyr}^{3'}$–H), 7.52 (2 H, ddd, *J* 1.5, 7.5 and 7.8, C_{pyr}^{4}–H and $C_{pyr}^{4'}$–H), 7.77 (2 H, bs, C^{3} and $C^{3'}$), 7.82 (2 H, d, *J* 8.2, C^{5}–H and $C^{5'}$–H), 7.93 (2 H, bs, C_{pyr}^{6}–H and $C_{pyr}^{6'}$–H) and 8.05 (2 H, d, *J* 8.0 Hz, C^{4}–H and $C^{4'}$–H); δ_C (75 MHz; solvent CD_2Cl_2) 64.5 (CH_2), 69.0 (CH_2), 119.9 (CH), 122.6 (C_{pyr}^{5} and $C_{pyr}^{5'}$), 124.9 (C^{3} and $C^{3'}$), 126.5 (C^{5} and $C^{5'}$), 127.1 (C^{6} and $C^{6'}$), 127.3 (C^{7} and $C^{7'}$), 128.4 (C^{8} and $C^{8'}$), 128.6 (C_{pyr}^{3} and $C_{pyr}^{3'}$), 129.6 (C^{4} and $C^{4'}$), 130.8 (quaternary C), 133.6 (quaternary C), 134.4 (quaternary C), 137.7 (quaternary C), 138.4 (C_{pyr}^{4} and $C_{pyr}^{4'}$), 153.3 (C_{pyr}^{6} and $C_{pyr}^{6'}$) and 161.5 (C_{pyr}^{2} and $C_{pyr}^{2'}$); δ_F (283 MHz, solvent CD_2Cl_2) −78.83 (CF_3); *m*/*z* (FAB+) 555 (82%) ($M - O_3SCF_3$), 514 (85) ($M - O_3SC_4F_3H_5$), 409 (100) and 330 (80). Complex (−)-**21** was prepared in identical manner from (−)-**6**: mp 166–168 °C, $[\alpha]_D$ (*c* = 0.10, CH_2Cl_2, 23 °C) = −168 deg cm^3 g^{-1} dm^{-1}.

Acknowledgements

G. C. L.-J. thanks the Zeneca Strategic Research Fund and Pfizer Ltd for generous support and N. J. H. AstraZeneca for an Industrial CASE award. The initial concept for this work arose from a discussion with Prof. Christoph J. Fahrni (Georgia Institute of Technology, USA) and we gratefully acknowledge his important contribution and encouragement. Dr Simon C. Woodward (University of Nottingham, UK) kindly provided details of his earlier work in the attempted preparation of ligand **6**.

References

1 See for example: *Catalytic Asymmetric Synthesis*, ed. I. Ojima, VCH Publishers, New York, 1993; *Asymmetric Catalysis in Organic Synthesis*, ed. R. Noyori, J. Wiley and Sons, New York, 1994; *Transition Metals for Organic Synthesis*, eds. M. Beller and C. Bolm, Wiley-VCH, Weinheim, 1998.
2 See for example, S. Akutagawa, in *Chirality in Industry*, eds. A. N. Collins, G. N. Sheldrake and J. Crosby, John Wiley & Sons, New York, 1992.
3 For leading references to semicorrin ligands see: A. Pfaltz, *Acc. Chem. Res.*, 1993, **26**, 339; C. Piqué, B. Fähndrich and A. Pfaltz, *Synlett*, 1995, 491.
4 For leading references to bis(oxazolines) see: D. A. Evans, J. S. Johnson, C. S. Burgey and K. R. Campos, *Tetrahedron Lett.*, 1999, **40**, 2879.
5 For leading references to bis(aziridine) ligands see: D. Tanner, F. Johansson, A. Harden and P. G. Andersson, *Tetrahedron*, 1998, **54**, 15731.
6 For related non-symmetric examples see H. Brunner, G. Olschewski and B. Nuber, *Synthesis*, 1999, 429.
7 Related ligands in which the donor groups are oxazolines (instead of pyridines) connected *via* C(2) to the 2,2′ positions of various biaryl compounds were reported by other groups during the present work. These ligands differ somewhat from **6** in that the oxazolines possess central chirality. See: Y. Uozomi, H. Kyota, E. Kishi, K. Kitayama and T. Hayashi, *Tetrahedron: Asymmetry*, 1996, **7**, 1603; T. G. Gant, M. C. Noe and E. J. Corey, *Tetrahedron Lett.*, 1995, **36**, 1831; M. B. Andrus, D. Asgari and J. A. Sclafani, *J. Org. Chem.*, 1997, **62**, 9365; A. J. Rippert, *Helv. Chim. Acta*, 1998, **81**, 676; Y. Imai, W. B. Zhang, T. Kida, Y. Nakatsuji and I. Ikeda, *Tetrahedron Lett.*, 1997, **38**, 2681.
8 Prepared from 2-naphthol by Fe-mediated oxidative dimerisation: R. Pummer, E. Prell and A. Rieche, *Chem. Ber.*, 1926, **59**, 2159.
9 H. Takaya, S. Akutagawa and R. Noyori, *Org. Synth.*, 1989, **67**, 20.
10 H. Gilman and J. T. Edwards, *Can. J. Chem.*, 1953, **31**, 457.
11 T. Kamikawa and T. Hayashi, *Tetrahedron Lett.*, 1997, **38**, 7087.
12 However, for some examples of recent catalysts that do allow chlorides to be used in high yielding Pd-catalysed cross-coupling, amination and Heck reactions, see: J. P. Wolfe, R. A. Singer, B. H. Yang and S. L. Buchwald, *J. Am. Chem. Soc.*, 1999; **121**, 9550; A. F. Littke and G. C. Fu, *J. Org. Chem.*, 1999, **64**, 10 and references therein.
13 M. Iyoda, H. Otsuka, K. Sato, N. Nisato and M. Oda, *Bull. Chem. Soc. Jpn.*, 1990, **63**, 80.
14 I. Colon and D. R. Kelsey, *J. Org. Chem.*, 1896, **51**, 2627.
15 For leading references see: L. Di Bari, G. Pescitelli and P. Salvadori, *J. Am. Chem. Soc.*, 1999, **121**, 7998; S. F. Mason, *Molecular Optical Activity and the Chiral Discriminations*, Cambridge University Press, Cambridge, 1982.
16 See for example: P. S. Pregosin and G. Trabesinger, *J. Chem. Soc., Dalton Trans.*, 1998, 727.
17 K. L. Granberg and J.-E. Bäckvall, *J. Am. Chem. Soc.*, 1992, **114**, 6858.
18 G. A. Morris and R. Freeman, *J. Magn. Reson.* 1978, **29**, 433.
19 J. W. Faller, M. J. Incorvia and M. E. Thomsen, *J. Am. Chem. Soc.*, 1969, **91**, 518.
20 We will report in detail on the full determination of the kinetics of the exchange process and other associated exchange processes arising from impurities (not present in the complex discussed herein), in due course: N. J. Hunt, G. C. Lloyd-Jones, M. Murray and T. Nowak, unpublished work.
21 A. Jutand and A. Mosleh, *J. Org. Chem.*, 1997, **62**, 261.
22 A. Gogoll, J. Örnebro, H. Grennberg and J.-E. Bäckvall, *J. Am. Chem. Soc.*, 1994, **116**, 3631.
23 SMART diffractometer control software, Bruker Analytical X-ray Instruments Inc., Madison, WI, 1998.
24 SAINT integration software, Bruker Analytical X-ray Instruments Inc., Madison, WI, 1998.
25 G. M. Sheldrick, SADABS, A program for absorption correction with the Siemens SMART system, University of Göttingen, 1996.